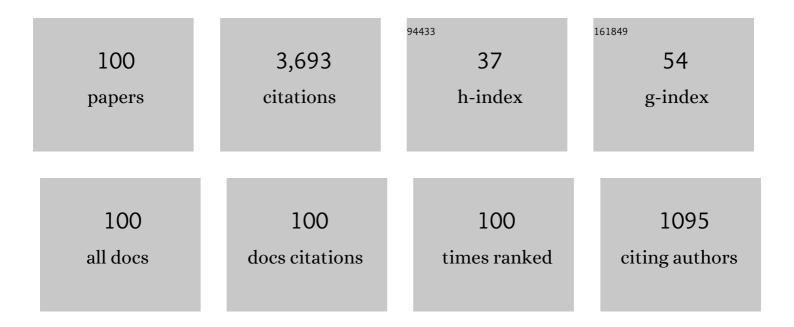
List of Publications by Year in descending order

Source: https://exaly.com/author-pdf/239929/publications.pdf Version: 2024-02-01



#	Article	IF	CITATIONS
1	Changes in permafrost extent and active layer thickness in the Northern Hemisphere from 1969 to 2018. Science of the Total Environment, 2022, 804, 150182.	8.0	30
2	Thermal control performance of the embankment with L-shaped thermosyphons and insulations along the Gonghe-Yushu Highway. Cold Regions Science and Technology, 2022, 194, 103428.	3.5	14
3	A hydraulic conductivity model of frozen soils with the consideration of water films. European Journal of Soil Science, 2022, 73, .	3.9	4
4	A self-adaption horizontal thermosyphon technology in uneven thermal control of roadway embankments in sub-arctic permafrost regions. Transportation Geotechnics, 2022, 33, 100714.	4.5	9
5	Study on the frost heave behavior of the freezing unsaturated silty clay. Cold Regions Science and Technology, 2022, 197, 103525.	3.5	20
6	A non-local frost heave model based on peridynamics theory. Computers and Geotechnics, 2022, 145, 104675.	4.7	5
7	Experimental study on the startup and heat transfer behaviors of a two-phase closed thermosyphon at subzero temperatures. International Journal of Heat and Mass Transfer, 2022, 190, 122283.	4.8	7
8	Rotational failure of concrete lining slabs induced by water level changes in ice-covered reservoirs in cold regions: Mechanism, patterns, and prevention measures. Cold Regions Science and Technology, 2022, 199, 103562.	3.5	4
9	Study on the solar albedo characteristics of pavement and embankment slope surfaces in permafrost regions. Solar Energy, 2022, 237, 352-364.	6.1	3
10	Engineering microbial systems for the production and functionalization of biomaterials. Current Opinion in Microbiology, 2022, 68, 102154.	5.1	5
11	Model tests of the barrier measures on moisture and salt migration in soils subjected to freeze-thaw cycles. Cold Regions Science and Technology, 2022, 201, 103607.	3.5	2
12	Multi-scale Experimental Investigations on the Deterioration Mechanism of Sandstone Under Wetting–Drying Cycles. Rock Mechanics and Rock Engineering, 2021, 54, 429-441.	5.4	25
13	Effect of freeze-thaw cycles on soil engineering properties of reservoir bank slopes at the northern foot of Tianshan Mountain. Journal of Mountain Science, 2021, 18, 541-557.	2.0	21
14	An integrated observation dataset of the hydrological and thermal deformation in permafrost slopes and engineering infrastructure in the Qinghai–Tibet Engineering Corridor. Earth System Science Data, 2021, 13, 4035-4052.	9.9	4
15	Experimental Study on the Effect of Freeze—Thaw Cycles on the Mineral Particle Fragmentation and Aggregation with Different Soil Types. Minerals (Basel, Switzerland), 2021, 11, 913.	2.0	16
16	Numerical optimization of the installing position for the L-shaped TPCT in a permafrost embankment based on the spatial heat control. Solar Energy, 2021, 224, 1406-1425.	6.1	8
17	Experimental study of optical and cooling performances of CuO and TiO2 near-infrared reflective blending coatings. Solar Energy, 2021, 225, 19-32.	6.1	12
18	Laboratory study on the frost-proof performance of a novel embankment dam in seasonally frozen regions. Journal of Hydrology, 2021, 602, 126769.	5.4	9

#	Article	IF	CITATIONS
19	Influence of nano-silica on the performances of concrete under the negative-temperature curing condition. Cold Regions Science and Technology, 2021, 191, 103357.	3.5	15
20	Variations of the temperatures and volumetric unfrozen water contents of fine-grained soils during a freezing–thawing process. Acta Geotechnica, 2020, 15, 595-601.	5.7	51
21	Variation behavior of pore-water pressure in warm frozen soil under load and its relation to deformation. Acta Geotechnica, 2020, 15, 603-614.	5.7	19
22	A generalized model for calculating the thermal conductivity of freezing soils based on soil components and frost heave. International Journal of Heat and Mass Transfer, 2020, 150, 119166.	4.8	30
23	Work conjugate stress and strain variables for unsaturated frozen soils. Journal of Hydrology, 2020, 582, 124537.	5.4	17
24	Countermeasures combined with thermosyphons against the thermal instability of high-grade highways in permafrost regions. International Journal of Heat and Mass Transfer, 2020, 153, 119047.	4.8	18
25	Investigation on frost heave of saturated–unsaturated soils. Acta Geotechnica, 2020, 15, 3295-3306.	5.7	43
26	Study on the coupled heat-water-vapor-mechanics process of unsaturated soils. Journal of Hydrology, 2020, 585, 124784.	5.4	41
27	Effect of length ratios on the cooling performance of an inclined two-phase closed thermosyphon under negative temperature conditions. Solar Energy, 2020, 204, 600-616.	6.1	18
28	Laboratory investigation of the efficiency optimization of an inclined two-phase closed thermosyphon in ambient cool energy utilization. Renewable Energy, 2019, 133, 1178-1187.	8.9	26
29	A black near-infrared reflective coating based on nano-technology. Energy and Buildings, 2019, 205, 109523.	6.7	24
30	Evaluation of the ground heat control capacity of a novel air-L-shaped TPCT-ground (ALTG) cooling system in cold regions. Energy, 2019, 179, 655-668.	8.8	63
31	Hydro-thermal behaviors of the ground under different surfaces in the Qinghai-Tibet Plateau. Cold Regions Science and Technology, 2019, 161, 99-106.	3.5	22
32	Hydro-thermal boundary conditions at different underlying surfaces in a permafrost region of the Qinghai-Tibet Plateau. Science of the Total Environment, 2019, 670, 1190-1203.	8.0	25
33	A developed method to measure and calculate the solar albedo of discrete-particle layers. Solar Energy, 2019, 194, 671-681.	6.1	4
34	Centrifuge and numerical modeling of the frost heave mechanism of a cold-region canal. Acta Geotechnica, 2019, 14, 1113-1128.	5.7	35
35	Thermal effect of rainwater infiltration into a replicated road embankment in a cold environmental chamber. Cold Regions Science and Technology, 2019, 159, 47-57.	3.5	10
36	Analysis of volumetric unfrozen water contents in freezing soils. Experimental Heat Transfer, 2019, 32, 426-438.	3.2	43

#	Article	IF	CITATIONS
37	A generalized thermal conductivity model of geomaterials based on micro-structures. Acta Geotechnica, 2019, 14, 1423-1436.	5.7	13
38	Experimental and theoretical studies on the solar reflectance of crushed-rock layers. Cold Regions Science and Technology, 2019, 159, 13-19.	3.5	10
39	Numerical evaluation of the cooling performance of a composite L-shaped two-phase closed thermosyphon (LTPCT) technique in permafrost regions. Solar Energy, 2019, 177, 22-31.	6.1	54
40	Thermo-seismic characteristics of a crushed-rock interlayer embankment on a permafrost slope. Cold Regions Science and Technology, 2018, 151, 249-259.	3.5	15
41	Experimental study on the freezing–thawing deformation of a silty clay. Cold Regions Science and Technology, 2018, 151, 19-27.	3.5	85
42	Experimental and numerical simulations on heat-water-mechanics interaction mechanism in a freezing soil. Applied Thermal Engineering, 2018, 132, 209-220.	6.0	72
43	Evaluation of calculation models for the thermal conductivity of soils. International Communications in Heat and Mass Transfer, 2018, 94, 14-23.	5.6	53
44	A new model to determine the thermal conductivity of fine-grained soils. International Journal of Heat and Mass Transfer, 2018, 123, 407-417.	4.8	53
45	Study on the freezing temperature of saline soil. Acta Geotechnica, 2018, 13, 195-205.	5.7	53
46	Experimental study of the hydro-thermal characteristics and frost heave behavior of a saturated silt within a closed freezing system. Applied Thermal Engineering, 2018, 129, 1447-1454.	6.0	28
47	Theory and application of a novel soil freezing characteristic curve. Applied Thermal Engineering, 2018, 129, 1106-1114.	6.0	66
48	Experimental study on the water-heat-vapor behavior in a freezing coarse-grained soil. Applied Thermal Engineering, 2018, 128, 956-965.	6.0	53
49	UAV-based spatiotemporal thermal patterns of permafrost slopes along the Qinghai–Tibet Engineering Corridor. Landslides, 2018, 15, 2161-2172.	5.4	13
50	Study of the time-dependent thermal behavior of the multilayer asphalt concrete pavement in permafrost regions. Construction and Building Materials, 2018, 193, 162-172.	7.2	17
51	A new simplified method for measuring the permeability characteristics of highly porous media. Journal of Hydrology, 2018, 562, 725-732.	5.4	85
52	The thermal effect of heating two-phase closed thermosyphons on the high-speed railway embankment in seasonally frozen regions. Applied Thermal Engineering, 2018, 141, 948-957.	6.0	39
53	Variation of the thermal conductivity of a silty clay during a freezing-thawing process. International Journal of Heat and Mass Transfer, 2018, 124, 1059-1067.	4.8	67
54	Water-vapor-heat behavior in a freezing unsaturated coarse-grained soil with a closed top. Cold Regions Science and Technology, 2018, 155, 120-126.	3.5	37

#	Article	IF	CITATIONS
55	Crack formation of a highway embankment installed with two-phase closed thermosyphons in permafrost regions: Field experiment and geothermal modelling. Applied Thermal Engineering, 2017, 115, 670-681.	6.0	64
56	Quantitative analysis for the effect of microstructure on the mechanical strength of frozen silty clay with different contents of sodium sulfate. Environmental Earth Sciences, 2017, 76, 1.	2.7	35
57	Effect of hydro-thermal behavior on the frost heave of a saturated silty clay under different applied pressures. Applied Thermal Engineering, 2017, 117, 462-467.	6.0	33
58	Water–heat migration and frost-heave behavior of a saturated silty clay with a water supply. Experimental Heat Transfer, 2017, 30, 517-529.	3.2	19
59	Crystallization deformation of a saline soil during freezing and thawing processes. Applied Thermal Engineering, 2017, 120, 463-473.	6.0	72
60	The Phase Change Process and Properties of Saline Soil During Cooling. Arabian Journal for Science and Engineering, 2017, 42, 3923-3932.	3.0	36
61	Theoretical and experimental studies on the daily accumulative heat gain from cool roofs. Energy, 2017, 129, 138-147.	8.8	106
62	Effect of Temperature Gradients on the Frost Heave of a Saturated Silty Clay with a Water Supply. Journal of Cold Regions Engineering - ASCE, 2017, 31, .	1.1	27
63	Model test study on the anti-saline effect of the crushed-rock embankment with impermeable geotextile in frozen saline soil regions. Cold Regions Science and Technology, 2017, 141, 86-96.	3.5	9
64	Estimating soil freezing characteristic curve based on pore-size distribution. Applied Thermal Engineering, 2017, 124, 1049-1060.	6.0	78
65	Geotemperature control performance of two-phase closed thermosyphons in the shady and sunny slopes of an embankment in a permafrost region. Applied Thermal Engineering, 2017, 112, 986-998.	6.0	52
66	Experimental and numerical analyses of the thermo-mechanical stability of an embankment with shady and sunny slopes in a permafrost region. Applied Thermal Engineering, 2017, 127, 1478-1487.	6.0	93
67	Thermo-mechanical stability analysis of cooling embankment with crushed-rock interlayer on a sloping ground in permafrost regions. Applied Thermal Engineering, 2017, 125, 1200-1208.	6.0	19
68	Enhancement of convective cooling of the porous crushed-rock layer in cold regions based on experimental investigations. International Communications in Heat and Mass Transfer, 2017, 87, 14-21.	5.6	24
69	Numerical study of the thermal characteristics of a shallow tunnel section with a two-phase closed thermosyphon group in a permafrost region under climate warming. International Journal of Heat and Mass Transfer, 2017, 104, 952-963.	4.8	53
70	A full-scale field experiment to evaluate the cooling performance of a novel composite embankment in permafrost regions. International Journal of Heat and Mass Transfer, 2016, 95, 1047-1056.	4.8	60
71	Typical embankment settlement/heave patterns of the Qinghai–Tibet highway in permafrost regions: Formation and evolution. Engineering Geology, 2016, 214, 147-156.	6.3	62
72	A naturally-occurring â€~cold earth' spot in Northern China. Scientific Reports, 2016, 6, 34184.	3.3	16

#	Article	IF	CITATIONS
73	Cooling performance of two-phase closed thermosyphons installed at a highway embankment in permafrost regions. Applied Thermal Engineering, 2016, 98, 220-227.	6.0	59
74	Experimental and numerical investigations on frost damage mechanism of a canal in cold regions. Cold Regions Science and Technology, 2015, 116, 1-11.	3.5	84
75	Seasonal differences in seismic responses of embankment on a sloping ground in permafrost regions. Soil Dynamics and Earthquake Engineering, 2015, 76, 122-135.	3.8	32
76	Heat and mass transfer effects of ice growth mechanisms in a fully saturated soil. International Journal of Heat and Mass Transfer, 2015, 86, 699-709.	4.8	60
77	Lateral thermal disturbance of embankments in the permafrost regions of the Qinghai-Tibet Engineering Corridor. Natural Hazards, 2015, 78, 2121-2142.	3.4	45
78	Evaluating the cooling performance of crushed-rock interlayer embankments with unperforated and perforated ventilation ducts in permafrost regions. Energy, 2015, 93, 874-881.	8.8	74
79	Effect of Inclination Angle on the Heat Transfer Performance of a Two-Phase Closed Thermosyphon under Low-Temperature Conditions. Journal of Cold Regions Engineering - ASCE, 2014, 28, .	1.1	30
80	Thermal stability analysis of crushed-rock embankments on a slope in permafrost regions. Cold Regions Science and Technology, 2014, 106-107, 175-182.	3.5	17
81	Study on theory model of hydro-thermal–mechanical interaction process in saturated freezing silty soil. International Journal of Heat and Mass Transfer, 2014, 78, 805-819.	4.8	215
82	Experimental study on ventilation characteristics of a concrete-sphere layer and a crushed-rock layer. International Journal of Heat and Mass Transfer, 2013, 59, 407-413.	4.8	28
83	Laboratory investigation of the heat transfer characteristics of a two-phase closed thermosyphon. Cold Regions Science and Technology, 2013, 95, 67-73.	3.5	26
84	A New Method to Determine the Upper Boundary Condition for a Permafrost Thermal Model: An Example from the Qinghaiâ€Tibet Plateau. Permafrost and Periglacial Processes, 2012, 23, 301-311.	3.4	15
85	Numerical analysis for thermal characteristics of cinderblock interlayer embankments in permafrost regions. Applied Thermal Engineering, 2012, 36, 252-259.	6.0	16
86	Numerical study on cooling characteristics of two-phase closed thermosyphon embankment in permafrost regions. Cold Regions Science and Technology, 2011, 65, 203-210.	3.5	86
87	Three-Dimensional Nonlinear Analysis for the Cooling Characteristics of Crushed-Rock Interlayer Embankment with Ventilated Duct along the Qinghai-Tibet Expressway in Permafrost Regions. Journal of Cold Regions Engineering - ASCE, 2010, 24, 126-141.	1.1	17
88	Numerical study on the influence of geometrical parameters on natural convection cooling effect of the crushed-rock revetment. Science in China Series D: Earth Sciences, 2009, 52, 539-545.	0.9	20
89	Seismic analysis of embankment of Qinghai–Tibet railway. Cold Regions Science and Technology, 2009, 55, 151-159.	3.5	25
90	Numerical study on temperature characteristics of expressway embankment with crushed-rock revetment and ventilated ducts in warm permafrost regions. Cold Regions Science and Technology, 2009, 59, 19-24.	3.5	51

#	Article	IF	CITATIONS
91	Laboratory investigation on cooling effect of duct-ventilated embankment with a chimney in permafrost regions. Cold Regions Science and Technology, 2008, 54, 115-119.	3.5	25
92	Experimental study on influence of particle size on cooling effect of crushed-rock layer under closed and open tops. Cold Regions Science and Technology, 2007, 48, 232-238.	3.5	40
93	Numerical analysis for random temperature fields of embankment in cold regions. Science in China Series D: Earth Sciences, 2007, 50, 404-410.	0.9	17
94	Influence of boundary conditions on the cooling effect of crushed-rock embankment in permafrost regions of Qinghai–Tibetan Plateau. Cold Regions Science and Technology, 2006, 44, 225-239.	3.5	77
95	A numerical model of the coupled heat transfer for duct-ventilated embankment under wind action in cold regions and its application. Cold Regions Science and Technology, 2006, 45, 103-113.	3.5	45
96	Experimental investigation on influence of boundary conditions on cooling effect and mechanism of crushed-rock layers. Cold Regions Science and Technology, 2006, 45, 114-121.	3.5	52
97	Laboratory investigation on cooling effect of sloped crushed-rock revetment in permafrost regions. Cold Regions Science and Technology, 2006, 46, 27-35.	3.5	38
98	Numerical analysis for cooling effect of open boundary ripped-rock embankment on Qinghai-Tibetan railway. Science in China Series D: Earth Sciences, 2006, 49, 764-772.	0.9	49
99	Laboratory Investigation of the Heat Transfer Characteristics of a Trapezoidal Crushed-Rock Layer Under Impermeable and Permeable Boundaries. Experimental Heat Transfer, 2006, 19, 251-264.	3.2	14
100	Nonlinear analysis for the cooling effect of Qinghai-Tibetan railway embankment with different structures in permafrost regions. Cold Regions Science and Technology, 2005, 42, 237-249.	3.5	63